Resonant hole polarons in GaAs and InP

J. N. Heyman, Nelson Coates,* Sheila Nabanja,† and Tobin Kaufman-Osborn
Department of Physics and Astronomy, Macalester College, Saint Paul, Minnesota 55105, USA

Fedir Kyrychenko
Department of Physics, University of Missouri, Columbia, Missouri 65211, USA
(Received 27 May 2008; revised manuscript received 28 July 2008; published 26 September 2008)

We use optically pumped time-domain measurements of cyclotron emission from GaAs and InP surfaces at $T=4.2$ K to determine electron light-hole and heavy-hole effective masses as functions of pump-photon energy. We observe both light-hole and electron-polaron resonances as resonant enhancements of the electron and hole masses when the kinetic energy of the carriers approaches the optical-phonon energy. In addition, our coherent terahertz measurements show that in our GaAs samples at low temperatures photoexcited electrons and holes initially accelerate in the same direction.

DOI: 10.1103/PhysRevB.78.125207 PACS number(s): 71.38.Fp, 76.40.+b, 78.47.J−

I. INTRODUCTION

Electron and hole effective masses in semiconductors vary with carrier energy due to band nonparabolicity and polaron effects. The variation in the curvature of the conduction and valence bands near the band extrema is well described by multiband $\mathbf{k}\cdot\mathbf{p}$ theory.[1] The polaronic shift of the carrier mass arises because a free carrier in a solid distorts the surrounding lattice. The coupled excitation is called a polaron and displays an enhanced effective mass relative to the bare mass determined by band curvature. In polar semiconductors the Fröhlich or polar-optical carrier-phonon interaction is dominant and the polaron coupling is weak and can be treated adequately using perturbation theory.[2] More sophisticated intermediate coupling theories have also been used to describe polar semiconductors and other materials. A review of the theory of Fröhlich polarons has recently been published.[3] Theory predicts a small increase in the electron effective mass at the conduction-band minimum $m^*=m_e/(1-\alpha_e/6)$, where m_e is the bare-electron effective mass, and the electron-polaron coupling coefficient $\alpha_e \ll 1$ with the coupling constant $\alpha_e^{(\mathrm{GaAs})}=0.08$ for GaAs while for InP $\alpha_e^{(\mathrm{InP})}=0.09$. Both perturbative and intermediate coupling theories predict a resonant enhancement of the effective mass when the electron energy approaches the optical-phonon energy. A similar polaron resonance has been predicted for holes in polar semiconductors over 30 years ago.[4] However, no clear evidence of a hole-polaron resonance has been reported until now.

Cyclotron absorption resonance measurements (CR) have been the primary tool for studying the carrier effective masses in semiconductors. Several studies[5–8] have investigated electron CR in n-GaAs and n-InP over the magnetic-field range $B=0-25$ T. Pulsed-field measurements[9] have investigated electron CR at fields up to $B=150$ T. Resonant enhancement of the electron effective mass is observed when the cyclotron frequency approaches the optical-phonon frequency. More generally, a resonant shift in the energy of the nth Landau level is observed[10] when $\omega_{\mathrm{LO}}/\omega_c=n$. These measurements have been successfully described using theories, which include both the conduction-band nonparabolicity and the polar electron-phonon interaction.[1,11,12] There have also been extensive measurements of electron CR in semiconductor heterostructures and quantum wells.[5] Magnetoluminescence has also been used to probe carrier effective mass[13] in GaAs heterostructures. Gubarev *et al.*[13] observed carrier-mass shifts due to nonparabolicity and resonant electron-phonon interaction in the magnetic-field dependence of the electron-light-hole exciton-luminescence line energies.

Cyclotron *emission* has also been observed in ultrafast terahertz-emission spectroscopy of semiconductors in magnetic fields.[14–16] Interband excitation with femtosecond laser pulses creates electrons and holes in a coherent superposition of Landau levels. Coherent terahertz emission is observed at the cyclotron frequencies of electrons, light holes, and heavy holes. By varying the pump-photon energy, one can control the kinetic energy of the carriers. Andrews *et al.*[16] reported a shift in electron-cyclotron emission peak when the electron excess energy equals the optical-phonon energy and interpreted this as evidence of the electron-polaron resonance. A detailed simulation of terahertz emission from electrons and holes in crossed electric and magnetic fields[17] describes many features of these data including variation in the cyclotron-emission amplitude and linewidth with excitation energy.

Few studies of the energy dependence of the hole effective mass in semiconductors have been reported. There are clear experimental challenges on studies of the polaron resonance of holes by cyclotron resonance. For example, the heavy-hole cyclotron frequency only reaches the optical-phonon frequency in GaAs at magnetic fields ~150 T. On the other hand, light-hole Landau levels are not populated at low temperatures and high magnetic fields making them inaccessible to equilibrium far-infrared-absorption measurements. By contrast, terahertz-emission measurements are not subject to this limitation because they probe a nonequilibrium distribution of carriers determined by the excitation pulse energy. Therefore terahertz emission is well suited to probing the variation in the hole effective mass with energy.

Both valence-band nonparabolicity and hole-polaron effects should contribute to the energy dependence of the hole effective mass. However polaron coupling for holes in zinc-blende semiconductors differs from that of electrons because

optical-phonon coupling causes transitions between the heavy- and light-hole bands. Beni and Rice[4] proposed a theory of hole polarons in zinc-blende semiconductors using second-order perturbation theory that includes mixing between the heavy- and light-hole bands. They predicted a polaronic mass shift for band-edge light holes 2.8 times larger than that yielded by a single-band treatment. This prediction has never been experimentally tested. Although the light- and heavy-hole masses at the valence-band maximum have been precisely measured in most III-V semiconductors, it has not been possible to predict the bare-hole masses with sufficient accuracy to determine the polaron shift. However, a strong test could be performed by measuring the variation in the light-hole mass near the polaron resonance.

In this work we report our time-domain terahertz cyclotron-emission measurements in GaAs and InP. We find significant variation in the electron light-hole and heavy-hole cyclotron effective masses with pump-photon energy, and we observe the electron and light-hole-polaron resonances in these materials. Our results are in good overall agreement with the theory proposed by Beni and Rice.

In addition, our coherent terahertz-emission measurements allow us to determine the relative phases of the electron and hole cyclotron emission as functions of time. Thus, we can compare the direction of motion of the two carrier species immediately following photoexcitation. A number of recent studies[18–21] have probed the mechanism whereby femtosecond interband excitation leads to a coherent transient current surge and terahertz emission in semiconductors. Most commonly, e.g., photoexcitation of an *n*-GaAs surface at room temperature by 1.5 eV femtosecond pulses, the strong surface Schottky electric field drives a polar transient photocurrent.[22] Under conditions where the surface electric field is weak and/or the carrier energies are high, photocarrier diffusion can drive an ambipolar current yielding a transient electric current if the electron and hole mobilities are not equal. Terahertz emission by hot-carrier diffusion is observed in terahertz emission from Te,[19] *n*-InAs,[18] InGaSb, and InSb (Ref. 20) following *fs* photoexcitation with 1.5 eV radiation and from GaAs at room temperature following photoexcitation with 3.1 eV optical pulses.[21] In this work, we unambiguously show that terahertz emission from our GaAs samples at 4.2 K arises from the motion of electron and holes with *parallel* initial velocities perpendicular to the sample surface. Apparently in these samples under strong illumination at low temperatures the initial impulsive excitation of the carriers is ambipolar.

II. EXPERIMENT

Our experiment used ultrafast terahertz spectroscopy to study optically pumped terahertz emission from GaAs and InP in a magnetic field. We primarily examined an epitaxial GaAs sample (G606) and bulk *n*-InP ($n \sim 7 \times 10^{15}$ cm^{-3}) as well as semi-insulating GaAs and InP:Fe samples. Sample G606 consisted of 1 μm undoped GaAs on 1 μm *n*-GaAs ($n = 1 \times 10^{17}$ cm^{-3}) grown on a semi-insulating substrate so that interband photoexcitation excites carriers into a region of uniform electric field. All samples were [001] oriented.

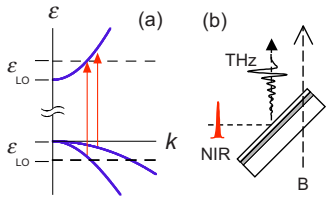

FIG. 1. (Color online) (a) Energy diagram showing interband excitation. Polaron resonance occurs when the carrier kinetic energy equals the energy of an optical phonon. (b) Experimental geometry. *fs*-NIR excitation pulses incident at 45° to sample surface and 90° to the **B** field. Terahertz emission recorded in pseudoreflection geometry.

The samples were excited with a mode-locked Ti-sapphire laser oscillator ($\tau \leq 12$ fs, $\lambda = 800$ nm, and $\Delta\lambda = 110$ nm). A tunable bandpass filter was used to obtain 0.02 eV full-width half-maximum bandwidth with ~120 fs pulses in the energy range $h\nu = 1.40 - 1.80$ eV. The excitation density at the sample was sufficiently low (~10 nJ/cm^2) such that the amplitudes of the terahertz pulses emitted were proportional to excitation intensity, and the terahertz pulse waveforms were independent of intensity.

The optical system comprised a time-domain terahertz-emission spectrometer. Terahertz pulses were generated at as-grown sample surfaces. Samples were mounted in an Oxford magneto-optical cryostat with quartz and polypropylene windows allowing optical access at near infrared (NIR) and terahertz wavelengths at magnetic fields up to 7 T. Preliminary measurements performed over a range of temperatures (300–5 K) were followed by systematic measurements with the sample in liquid helium at 4.2 K. The measurement geometry is shown in Fig. 1. The pump beam was incident on the sample surface at 45°. The magnetic field was parallel to the reflected pump beam and at 45° to the sample surface. Terahertz-emission measurements were performed in the pseudoreflection geometry, and the terahertz radiation emitted from the sample was focused onto a detector using two off-axis parabolic mirrors. Electron and light-hole cyclotron-emission measurements used a 1-mm-thick ⟨110⟩ ZnTe electro-optic terahertz detector ($0.1 < f < 3$ THz). We obtained enhanced sensitivity at low frequencies ($f < 0.5$ THz) by using a photoconductive antenna terahetz detector (DelMar Photonics) to study heavy-hole cyclotron emission. We used the polarization sensitivity of these detectors to independently measure the transverse electric (TE or *S*) and transverse magnetic (TM or *P*) components of the terahertz emission.

III. RESULTS

Initial measurements investigated terahertz emission from an epitaxial GaAs (G606) sample at $B = 0 - 4$ T at temperatures between 300 and 4.2 K. For $T > 100$ K the waveform amplitude and shape were only weakly temperature dependent. As the temperature was decreased from 100 to 90 K the integrated spectral amplitude decreased by approximately one order of magnitude. Clear electron-cyclotron oscillations ($\omega_c \tau > 1$) were observed for $T < 50$ K, and the electron

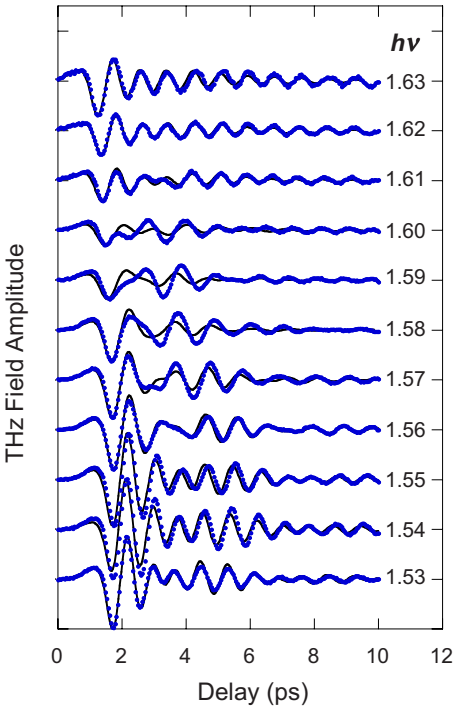

FIG. 2. (Color online) Terahertz emission from G606 (GaAs) at $\mathbf{B}=3$ T and $T=4.2$ K versus pump-photon energy normalized for pump power. Waveforms are offset for clarity. Dots are experimental data and solid lines are fits to our semiclassical model.

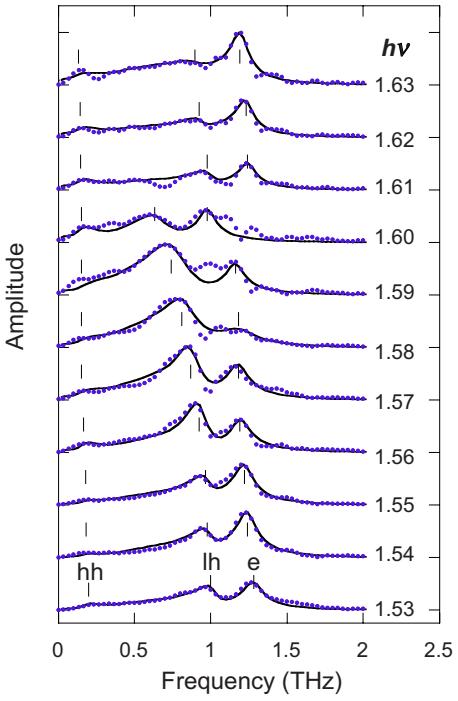

FIG. 3. (Color online) Terahertz-emission amplitude versus frequency from G606 (GaAs) at $\mathbf{B}=3$ T and $T=4.2$ K versus pump-photon energy normalized for pump power. Dots are experimental data and solid lines are fits to our semiclassical model. Upright slashes show best-fit cyclotron frequencies.

dephasing time increased to $\tau\sim 3$ ps at $T=4.2$ K. The spectrally integrated power was approximately temperature independent for $T<75$ K. We tentatively associate the tenfold signal decrease between 100 and 90 K with photocarrier trapping at the surface leading to screening of the surface electric field.

At $T=4.2$ K and magnetic fields of 1–6 T the terahertz emission from the as-grown G606 sample can be described well as a superposition of three damped sinusoidal waves. The frequencies of the sinusoidal components are proportional to magnetic field and can be identified as coherent cyclotron emission from photoexcited electrons, light holes, and heavy holes. The cyclotron emission shows a striking dependence on excitation energy (Fig. 2). Its Fourier transform (the spectral amplitude) measured for near band-gap excitation (1.53 eV) shows distinct electron light-hole and heavy-hole cyclotron resonance peaks (Fig. 3). As the excitation energy is increased to 1.58 eV the electron-cyclotron resonance feature shifts to lower frequency. The peak shape becomes more complex for excitation energies of 1.58–1.60 eV. At higher excitation energies the electron-cyclotron feature is recovered near its initial frequency. The light-hole peak shows a strong dependence on excitation energy shifting to lower frequency as the excitation energy is increased—broadening and growing in amplitude. The shape of the feature becomes complex for excitation energies near 1.60 eV, and weak light-hole feature shifts back to higher frequencies for excitation energies above 1.61 eV. Data obtained at $B=2$, 4, and 6 T similarly show distinct cyclotron peaks on a broad background with shifts in the cyclotron resonance frequencies with increasing excitation energy. The heavy-hole cyclotron resonance frequency in GaAs is also observed to shift to lower frequencies with increasing pump-photon energy.

We also observe terahertz cyclotron emission from the n-InP sample, although the dephasing times at $T=4.2$ K in this sample were only $\tau\sim 1.5$ ps. The excitation energy dependence is qualitatively similar to GaAs. The electron-cyclotron frequency shifts to lower frequency as the pump-photon energy is increased to $h\nu=1.50$ eV and shifts to lower frequencies for $h\nu>1.51$ eV. The light-hole emission shifts strongly to lower frequencies as the photon energy is increased to $h\nu=1.54$ eV and then shifts to lower frequencies. We were not able to resolve heavy-hole cyclotron emission from this sample due to the rapid dephasing.

IV. DISCUSSION: POLARON RESONANCE

We observe large shifts in cyclotron frequency when the carrier kinetic energies approach the optical-phonon energy (Fig. 3). In interband optical transitions the photon energy determines the energy of the electrons and holes. For transitions from the light-hole band to the conduction band, $h\nu-E_G=\varepsilon_k^e+\varepsilon_k^{\mathrm{LH}}$, where ε_k^e and $\varepsilon_k^{\mathrm{LH}}$ are the electron and light-hole energies at wave vector k, and we neglect the momentum of the photon. In GaAs at $T=4$ K, we expect $\varepsilon_k^e=\varepsilon_{\mathrm{LO}}$ when $h\nu=1.58$ eV and $\varepsilon_k^{\mathrm{LH}}=\varepsilon_{\mathrm{LO}}$ when $h\nu=1.60$ eV, while in InP, $\varepsilon_k^e=\varepsilon_{\mathrm{LO}}$ when $h\nu=1.50$ eV and $\varepsilon_k^{\mathrm{LH}}=\varepsilon_{\mathrm{LO}}$ when $h\nu=1.53$ eV.

To further analyze our results we use an empirical semiclassical model to extract electron and hole masses from our

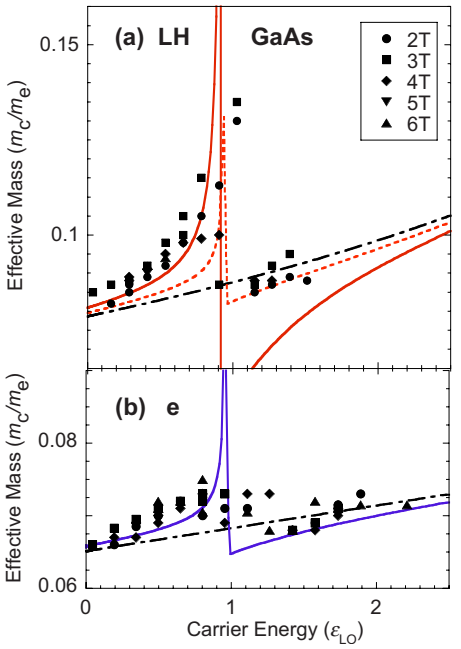

FIG. 4. (Color online) Measured (a) light hole and (b) electron cyclotron effective masses in GaAs versus carrier energy in units of the optical-phonon energy (symbols). Dash-dotted lines are bare masses calculated from an eight-band $\mathbf{k}\cdot\mathbf{p}$ theory. Solid lines include polaron coupling, while dashed line includes polaron coupling with no mixing between light and heavy holes.

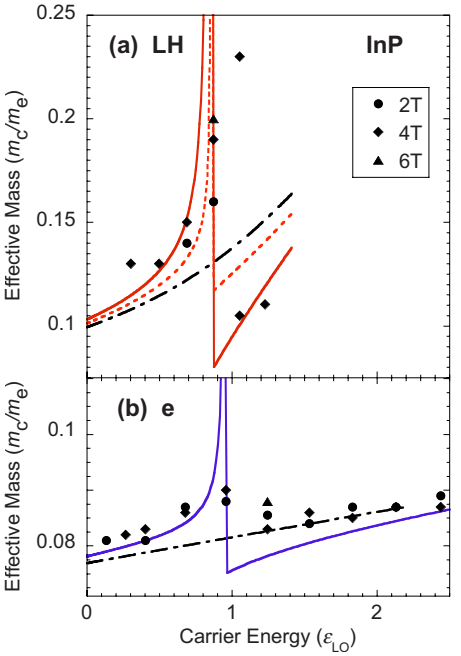

FIG. 5. (Color online) Measured (a) light hole and (b) electron cyclotron effective masses in InP versus carrier energy in units of the optical-phonon energy (symbols). Dash-dotted lines are bare masses calculated from an eight-band $\mathbf{k}\cdot\mathbf{p}$ theory. Solid lines include polaron coupling, while dashed line includes polaron coupling with no mixing between light and heavy holes.

cyclotron-emission measurements. We compare these to bare carrier masses obtained from eight-band $\mathbf{k}\cdot\mathbf{p}$ model and to modified carrier masses, which include a polaron correction to the effective mass obtained from second-order perturbation theory.

In the semiclassical model, we assume impulsive excitation and calculate carrier trajectories by integrating the equations of motion,

$$m_i\mathbf{a}_i = q_i(\mathbf{E} + v_i \times \mathbf{B}) - m_i\mathbf{v}_i/\Gamma_i, \tag{1}$$

where m_i is the effective mass and Γ_i is an effective scattering rate for the ith carrier type. We use the calculated carrier trajectories to calculate the time-dependent dipole moment and the radiated terahertz waveform. The effective masses, initial velocities and carrier scattering rates are taken as adjustable parameters and varied to obtain the best fit to the time-domain waveform. The simulated waveforms and spectra for $B=3$ T are shown in Figs. 2 and 3. The model describes the data well, although significant discrepancies are observed at $h\nu=1.59$ eV and 1.60 eV near the electron and light-hole-polaron resonances. Markers show the best-fit cyclotron frequencies for each excitation spectrum in Fig. 3.

We note two limitations of this treatment. The semiclassical approximation simplifies our analysis by ignoring the quantization of the energy bands into Landau subbands. This is valid when the Landau-level spacing is small compared to the energy bandwidth of our excitation pulses, i.e., at low magnetic fields. However, at $B=6$ T the bandwidth of our excitation pulses is only two times the electron-cyclotron energy. In addition, to compare model results with the measured waveforms, we must account for propagation effects in our optical system. We do this by convolving the model waveforms with the impulse response function of our terahertz system, which we determine experimentally by measuring the waveform generated by our sample at room temperature and zero magnetic field, where the carrier scattering rate is much larger than the bandwidth of our terahertz spectrometer. In practice, this correction plays a minor role in analyzing the data presented here.

In both GaAs and InP samples, we find that the electron and light-hole effective masses extracted using our semiclassical model are dependent on the kinetic energy of the carriers (Figs. 4 and 5) and show a resonant shift when the kinetic energy approaches the optical-phonon frequency. The shift in light-hole mass is much larger than the corresponding shift in electron mass: In GaAs the resonant shift in light-hole mass is ~50% of the unperturbed mass compared to a ~10% shift in electron mass.

We compare our experimental carrier masses to a theoretical model that includes both band nonparabolicity and polaron effects. To simulate the band structure of our samples we employ an eight-band $\mathbf{k}\cdot\mathbf{p}$ approach[23] that accounts for anisotropy and nonparabolicity of electron and hole bands. The model parameters are given in Table I. We used these results to calculate the bare cyclotron masses for electrons and holes as a function of carrier kinetic energy,

$$m_c = \frac{\hbar}{2\pi}\oint \frac{k}{\partial E/\partial k}d\phi, \tag{2}$$

where the integral is over a constant energy contour in k space. For electrons and light holes, band warping is rela-

TABLE I. Model parameters taken from Ref. 1.

Parameter	GaAs	InP
Energy gap E_G (eV)	1.519	1.423
Spin-orbit splitting Δ (eV)	0.341	0.108
Interband matrix element E_P (eV)	27.86	20.93
Electron mass m_e	0.065	0.077
Luttinger parameters		
γ_1	6.97	6.26
γ_2	2.25	2.08
γ_3	2.85	2.75

tively unimportant so that cyclotron masses calculated from spherical nonparabolic bands agree closely with those obtained including warping. For heavy holes band warping is significant.

Beni and Rice used second-order perturbation theory to calculate the hole-polaron self-energy in zinc-blende semiconductors. They obtained an expression for the polaron correction to the carrier self-energies for valence-band holes in the spherical Luttinger approximation,

$$\Sigma^{\mathrm{LH,HH}}(\mathbf{k},\varepsilon_{\mathbf{k}}^{\mathrm{LH,HH}}) = \sum_q |M_q|^2 \left[\frac{1/2(1+3\cos^2\theta)}{\varepsilon_{\mathbf{k}}^{\mathrm{LH,HH}} - \varepsilon_{\mathbf{k-q}}^{\mathrm{LH,HH}} - \hbar\omega_{\mathrm{LO}}} + \frac{3/2\sin^2\theta}{\varepsilon_{\mathbf{k}}^{\mathrm{LH,HH}} - \varepsilon_{\mathbf{k-q}}^{\mathrm{HH,LH}} - \hbar\omega_{\mathrm{LO}}} \right], \quad (3)$$

where the matrix element

$$|M_q|^2 = \frac{e^2\hbar\omega_{\mathrm{LO}}}{2q^2}[\varepsilon_\infty^{-1} - \varepsilon_0^{-1}],$$

and $\varepsilon_{\mathbf{k}}^{\mathrm{LH,HH}}$ is the kinetic energy of the light or heavy hole. Here θ is the angle between the hole wave vector $\mathbf{k}$ and the phonon wave vector $\mathbf{q}$, while ε_0 and ε_∞ are the static and optical dielectric constants, respectively. The second term on the right-hand side of Eq. (3) comes from mixing of the light- and heavy-hole bands due to the polar-optical hole-phonon interaction. We used Eq. (3) to calculate the polaron correction for spherically averaged nonparabolic electron and hole bands. We then used Eq. (2) to calculate the cyclotron mass for the corrected electron and light-hole bands.

We compare the resulting calculated electron and light-hole effective masses for GaAs and InP obtained from this theory with our measured cyclotron masses in Figs. 4 and 5. The theoretical treatment has no adjustable parameters. Agreement with experiment is good for carrier energies below the optical-phonon energy. First, the theory predicts the resonant shift in the light-hole and electron masses at carrier energies near the optical-phonon energy observed in our measurements. Second, the predicted polaron correction to the light-hole effective mass is substantially larger than that of the electrons in agreement with measurement. In contrast, light-hole-polaron masses calculated without including mixing between light and heavy holes underestimate the experimental masses in GaAs. However, the model predicts a divergence in the carrier effective masses at resonance that is not observed. In addition, the model significantly underestimates the light-hole mass in GaAs for carrier energies above the optical-phonon energy. These discrepancies may arise from the limitations of the model. Perturbation theory is likely to break down close to resonance, particularly because the theory does not include carrier or phonon scattering. In addition, uncertainty in the experimental photocarrier energies due to the bandwidth of the excitation pulse (0.02 eV) may artificially broaden the measured shape of the resonance.

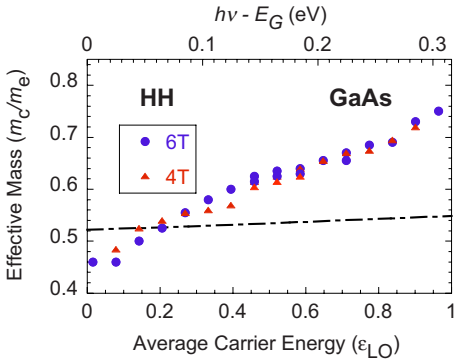

FIG. 6. (Color online) Measured heavy-hole cyclotron effective mass versus average carrier energy in units of the optical-phonon energy in GaAs (sample G606) (symbols). The optical excitation energy above band gap is shown in the upper x axis. Dash-dotted line is the bare heavy-hole cyclotron mass calculated from an eight-band $\mathbf{k}\cdot\mathbf{p}$ theory.

Figure 6 shows the heavy-hole mass in GaAs versus average kinetic and excitation energies. The heavy-hole mass increases monotonically from $m_{\mathrm{hh}}=0.46m_0$ at $h\nu=E_G$ to $m_{\mathrm{hh}}=0.72m_0$ at $h\nu=E_G+0.3$ eV and shows no distinct resonant feature within this range. We also plot the bare heavy-hole cyclotron mass predicted from our eight-band $\mathbf{k}\cdot\mathbf{p}$ model using Eq. (2). In the model, heavy-hole mass variation arises from band nonparabolicity. The model overestimates the heavy-hole mass at low kinetic energies by ~12%. The measured variation in the heavy-hole cyclotron mass is much larger than that observed in the model, and we suggest that this is due to polaron coupling. However, we have not attempted to model the polaron self-energy of the heavy holes due to the substantial warping of the heavy-hole band, which is not treated by Beni and Rice. In addition, the heavy-hole distribution probed in our experiment is not monoenergetic: Electron-hole pairs created by interband absorption at a given photon energy may have heavy-hole energies as much as ~20% larger or smaller than the average energy due to band warping. Clearly, this effect may smear out any resonant feature in the heavy-hole mass.

V. DISCUSSION: INITIAL CARRIER VELOCITIES

In both GaAs and InP, our terahertz-emission waveforms show beating between electron and light-hole cyclotron emissions, which are pronounced when the electron and light-hole signals have similar amplitude (Fig. 7). In G606 and in our SI-GaAs samples we observed an antinode in the beating pattern near zero delay in the TE (or S-polarized)

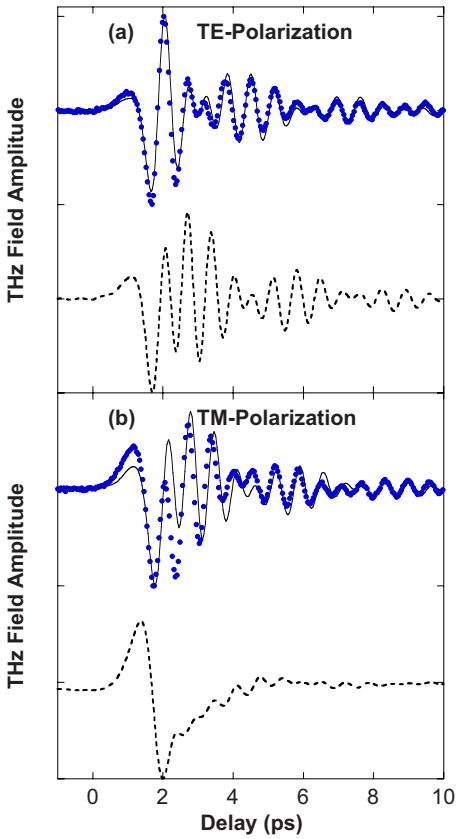

FIG. 7. (Color online) Terahertz emission from GaAs (sample G606) at $\mathbf{B}=4$ T, $T=4.2$ K, and pump-photon energy $h\nu=1.54$ eV showing beating between electron and light-hole cyclotron emissions. (a) TE (S)-polarized terahertz emission. (b) TM (P)-polarized terahertz emission. Dots are experimental data. Solid lines are a model fit with parallel initial electron, light-hole velocities, and $\mathbf{E}=0$. Dashed lines (offset for clarity) are a model fit with zero initial carrier velocities and finite-surface electric field.

component of the signal and a node near zero delay in the TM (or P-polarized) component.

Analysis of the beating observed between electron and light-hole cyclotron radiations allows us to determine the relative initial phase of the electron and hole cyclotron motions. Qualitatively, an oscillating dipole moment parallel to the plane of incidence produces TM radiation while one oscillating perpendicular produces TE radiation. We assume the initial carrier velocities are perpendicular to the surface and lie in the plane of incidence. If the electron and light-hole initial velocities have the same initial direction, their contributions to TM component of the terahertz waveform will initially cancel giving a node in the beating pattern near zero delay, while opposite initial velocities would give an antinode. Since the circular cyclotron motions of the electrons and holes have opposite handedness, the situation is reversed for the TE component of the waveform. The beating pattern we observe in our GaAs samples is consistent with parallel initial carrier velocities.

Using the semiclassical model described above, we can get an excellent quantitative fit to both the TE and TM components of the waveforms from G606 (GaAs) when we assume an ambipolar impulsive excitation and set the electron and hole initial velocities parallel to each other. In contrast setting the initial carrier velocities to zero and adding a finite electric field gives a poor fit with the pattern of nodes and antinodes in the model waveform opposite to that observed. Moreover, in the latter case the TM component of the model waveform is dominated by purely damped carrier motion parallel to the magnetic field because the electric field separates electron and holes to create a large dipole moment parallel to **B**. This is not observed in the experimental data. We conclude that in sample G606 at low temperatures the terahertz emission is powered by an ambipolar mechanism rather than by a surface electric field. Two well-known mechanisms that produce ambipolar carrier transport are the photocarrier diffusion and the photon-drag effect,[24] which emerges when we conserve both photon energy and momentum in the absorption process.

VI. CONCLUSIONS

We have used time-domain terahertz emission from GaAs and InP in a magnetic field to investigate cyclotron emission from electrons, light holes, and heavy holes. Emission measurements performed as functions of excitation energy allowed us to determine the carrier masses as functions of energy. In particular, we report an observation of the polaron resonance for light holes in III-V semiconductors. We model our results using energy bands obtained from an eight-band $\mathbf{k}\cdot\mathbf{p}$ band-structure calculation and a polaronic correction to the band energies obtained from second-order perturbation theory. The theory successfully predicts the electron and light-hole-polaron resonances as well as the enhancement of polaronic shift of the light-hole mass predicted due to mixing of the light- and heavy-hole bands.

In addition, our coherent-emission measurements allow us to determine the initial phase of the electron and hole cyclotron oscillations and thus compare the initial velocities of electrons and light holes. We find that in our GaAs samples at low temperatures photoexcited electrons and holes initially accelerate in the same direction. This is consistent with an ambipolar excitation mechanism such as hot-carrier diffusion or photon drag but is inconsistent with carrier acceleration in a surface electric field.

ACKNOWLEDGMENTS

G. Strasser of the Vienna University of Technology provided the epitaxial samples used in these measurements. We also thank J. Devreese for his comments on the draft of this paper. This work was supported by the National Science Foundation through the NSF-RUI program (Grants No. DMR-0317276 and No. DMR-0606181).

*Present address: Department of Physics, University of California at Santa Barbara, California 93106.
†Present address: Department of Electrical Engineering, Massachusetts Institute of Technology, Cambridge, Massachusetts 02139.

[1] P. Pfeffer and W. Zawadzki, Phys. Rev. B **53**, 12813 (1996).
[2] H. Fröhlich, H. Pelzer, and S. Zienau, Philos. Mag. **41**, 221 (1950).
[3] J. T. Devreese, J. Phys.: Condens. Matter **19**, 255201 (2007).
[4] G. Beni and T. M. Rice, Phys. Rev. B **15**, 840 (1977).
[5] H. Sigg, P. Wyder, and J. A. A. J. Perenboom, Phys. Rev. B **31**, 5253 (1985).
[6] G. Lindemann, R. Lassnig, W. Seidenbusch, and E. Gornik, Phys. Rev. B **28**, 4693 (1983).
[7] M. A. Hopkins, R. J. Nicholas, P. Pfeffer, W. Zawadzki, D. Gauthier, J. C. Portal, and M. A. DiForte-Poisson, Semicond. Sci. Technol. **2**, 568 (1987).
[8] H. Kobori, T. Nomura, and T. Ohyama, Phys. Rev. B **63**, 115201 (2001).
[9] S. P. Najda, S. Takeyama, N. Miura, P. Pfeffer, and W. Zawadzki, Phys. Rev. B **40**, 6189 (1989).
[10] C. M. Hu, E. Batke, K. Köhler, and P. Ganser, Phys. Rev. Lett. **76**, 1904 (1996).
[11] P. Pfeffer and W. Zawadzki, Phys. Rev. B **37**, 2695 (1988).
[12] G.-Q. Hai and F. M. Peeters, Phys. Rev. B **60**, 16513 (1999).
[13] S. I. Gubarev, T. Ruf, M. Cardona, and K. Ploog, Phys. Rev. B **48**, 1647 (1993).
[14] D. Some and A. V. Nurmikko, Phys. Rev. B **50**, 5783 (1994).
[15] D. Some and A. V. Nurmikko, Phys. Rev. B **53**, R13295 (1996).
[16] S. R. Andrews, A. Armitage, P. G. Huggard, C. J. Shaw, and G. P. Moore, Appl. Phys. Lett. **66**, 085307 (2002).
[17] M. B. Johnston, D. M. Whittaker, A. Corchia, A. G. Davies, and E. H. Linfield, Phys. Rev. B **65**, 165301 (2002).
[18] P. Gu, M. Tani, S. Kono, K. Sakai, and X.-C. Zhang, J. Appl. Phys. **91**, 5533 (2002).
[19] T. Dekorsy, H. Auer, H. J. Bakker, H. G. Roskos, and H. Kurz, Phys. Rev. B **53**, 4005 (1996).
[20] R. Ascazubi, I. Wilke, K. J. Kim, and P. Dutta, Phys. Rev. B **74**, 075323 (2006).
[21] J. N. Heyman, N. Coates, and A. Reinhardt, Appl. Phys. Lett. **83**, 5476 (2003).
[22] X. C. Zhang, B. B. Hu, J. T. Darrow, and D. H. Auston, Appl. Phys. Lett. **56**, 1011 (1990).
[23] G. L. Bir and G. E. Pikus, *Symmetry and Strain-Induced Effects in Semiconductors* (Wiley, New York, 1974).
[24] R. Loudon, S. M. Barnett, and C. Baxter, Phys. Rev. A **71**, 063802 (2005).